

Flow measurements through fluctuating interfaces with dynamic wavefront correction

Hannes Radner*, Lars Büttner, Jürgen Czarske

TU Dresden, Faculty of electrical and computer engineering, Laboratory for Measurement and Sensor System Technique, Dresden, Germany

*hannes.radner@tu-dresden.de

Abstract

Droplets play an important role in chemical industry, since they offer a large contact surface for the reaction between chemical substances. These reactions can be further improved with a deeper insight of the flow field, the concentration of the chemicals and temperature in and outside of the droplet. Laser optical measurement techniques measure contactless and offer a high resolution. However, optical measurements can be significantly degraded by the refractive index change at the fluctuating interface. For instance in Particle Tracking Velocimetry (PTV) and Particle Imaging Velocimetry (PIV) the fluctuating interface leads to a wrong localization of the particles. The fluctuation adds a virtual turbulence and increases the standard deviation of the mean flow. A constant distortion adds a systematic deviation to the flow field. Static distortions can easily be calibrated but unknown time-varying distortions not. In this paper, we present a novel technique for dynamic wavefront correction. This technique employs a wavefront sensor for measuring the distortion, a control loop and an adaptive optical element for the correction. Here we consider the fluctuations of an open water surface induced by an air flow. The system is able to suppress dynamic distortions with up to 200 Hz. We can show, that the standard deviation of a Particle Image Velocimetry (PIV) flow measurement behind a fluctuating water-air interface can be significantly reduced by 47 % with this system.

1 Introduction

Droplets and bubbles are important for efficient chemical reactions, because they have a large surface compared to their volume. To improve the reactions, knowledge about the flow field, temperature distribution and concentration of the chemicals is necessary. Laser optical measurement techniques could be used to measure these values. However, they need an undisturbed optical path between the system and the measurement volume. In some setups this requirement can not be fulfilled because significant refractive index fluctuations disturb the wavefront. These disturbances can be classified in general in volumetric distortions and phase boundary distortions. Volumetric distortions occur for example in tissues or combustion chambers with high temperature and pressure gradients Schlüßler et al. (2014) Willert et al. (2006). Phase boundary distortions occur at an interface between two media with different refractive indexes e.g. a fluctuating water-air interface. To correct optical distortions, wavefront correction systems were developed. The basic concept is shown in fig. 1. A laser is used to generate a guide star, which emits well known wavefronts. These are distorted similar as the light from the measurement volume. A wavefront sensor can measure this distortion and a control system steers an adaptive optical element to compensate the distortion. This concept was successfully adapted for metrology tasks Büttner et al. (2014) Büttner et al. (2013) Radner et al. (2018b) Radner et al. (2015) Radner et al. (2018a). For many applications, a fast wavefront correction is important. For instance, an air stimulated fluctuating interface of a 20 μl droplet fluctuates with up to 177 Hz Burgmann et al. (2017). To meet this challenge we present a custom tailored Field Programmable Gate Array (FPGA) system in combination with a fast deformable mirror and wavefront sensor. This system is able to suppress distortions of up to 200 Hz.

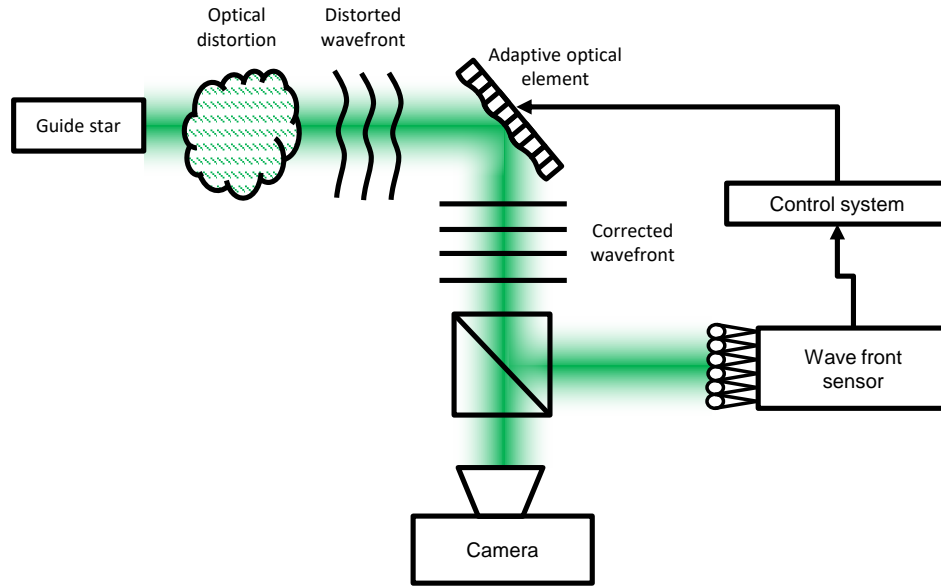


Figure 1: Basic concept of an adaptive optical wavefront correction system.

2 Setup

The setup is shown in fig. 2. It consists of a basin filled with water, where a flow can be generated behind a nozzle. The open water surface can be excited by an air flow to induce an optical distortion. The water flow behind the nozzle is not affected by the induced distortion nor does the water flow contribute to the surface fluctuation. The particles are illuminated with a laser light sheet with $\lambda_2 = 660 \text{ nm}$ from the side. The

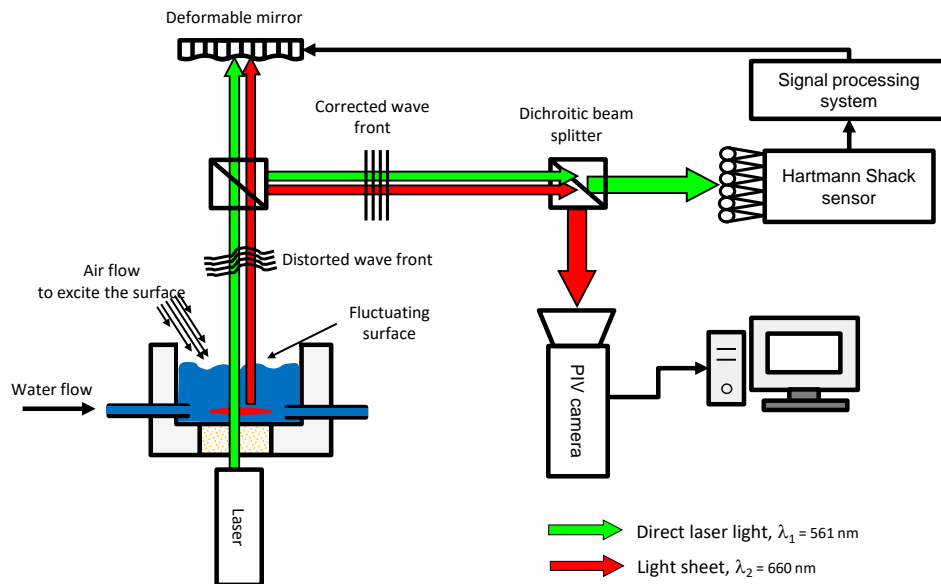


Figure 2: PIV setup with an in-house developed wavefront correction system.

green laser $\lambda_1 = 561 \text{ nm}$ serves as a guide star and samples the fluctuating surface. A dichroic beamsplitter separates the guide star light and the light from the particles for the PIV evaluation. An in-house developed high-speed Hartmann-Shack wavefront sensor measures the distortion. The sensor consists of a micro lens array with a CMOS chip placed at the focal plane of the array, see fig. 3(a). A local tilt of the incoming wavefront leads to a shift of the focal spot on the CMOS sensor. With a calibrated decomposition matrix

the shift of all spots can be decomposed into a superposition of Zernike polynomials. Zernike polynomials form an orthonormal base and a linear combination of them can be used to describe wavefront distortions. The signal processing system tries to display the inverse distortion on a fast deformable membrane mirror (Alpao DM69) to compensate the distortion. The mirror consists of a metallic membrane which is actuated by 69 pistons from the bottom, see fig. 3(b). The pistons have an attached magnet and a force can be applied by a current flow through the electric coil. The complete control system achieves a control rate of up to 2500 Hz and can suppress distortions of up to 200 Hz.

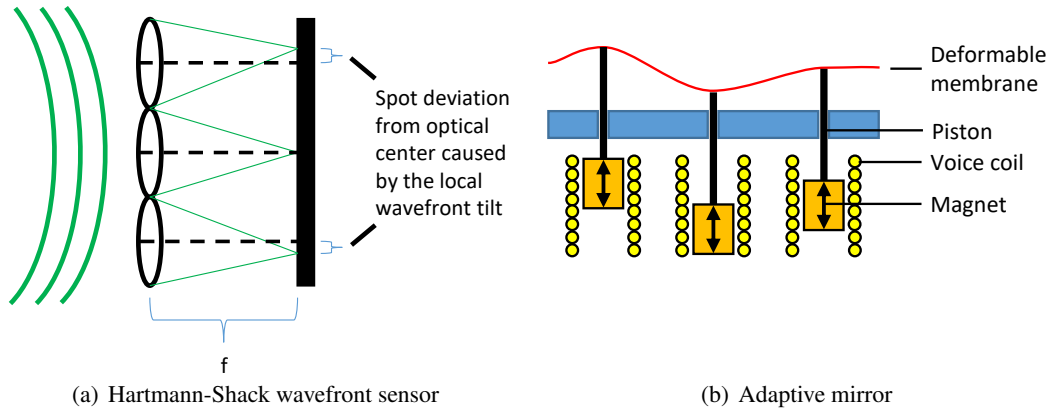


Figure 3: Components of the wavefront correction system: 3(a) The Hartmann-Shack wavefront sensor consists of a micro-lens array where a CMOS sensor is placed in the focal plane. A tilt of the local wavefront leads to a deviation of the spot on the CMOS sensor from the optical center. 3(b) The adaptive mirror (Alpao DM69) consists of a metallic membrane, which is attached to 69 pistons on the bottom side. A magnet is attached to the pistons and an electric coil can apply force to it.

The control loop can be modeled as shown in fig. 4. The distorted wavefront y is measured by Hartmann-Shack wavefront sensor. After an image correction the position y_z of all spots on the CMOS is determined. The positions are subtracted by a reference position r , which corresponds to a plane wavefront. The deviation e is decomposed into a linear combination of k Zernike polynomials which are feed into a controller. The controller sets the needed set value u to the adaptive mirror.

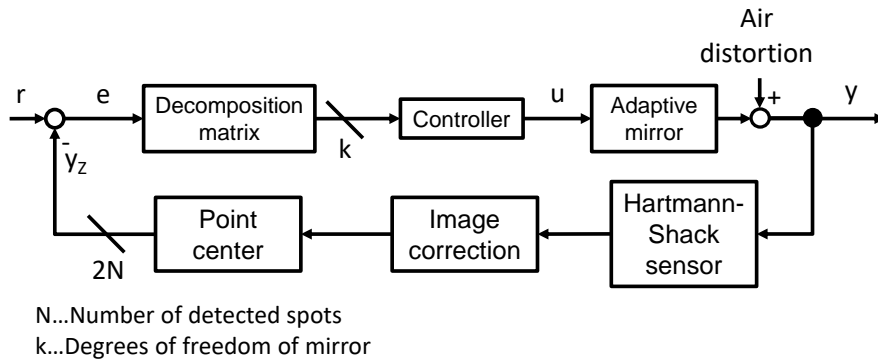


Figure 4: Scheme of the control loop. A Hartmann-Shack wavefront sensor measures the distorted wavefront. The position of the spots on the Hartmannogramm y_z is compared with reference positions r corresponding to a plane wavefront. The deviation is decomposed into low order Zernike polynomials which are feed into a controller that controls the mirror.

3 Results

The air induced distortion is characterized in fig. 5. It can be seen, that the surface fluctuates with up to 170 Hz for Zernike Noll-index Z7.

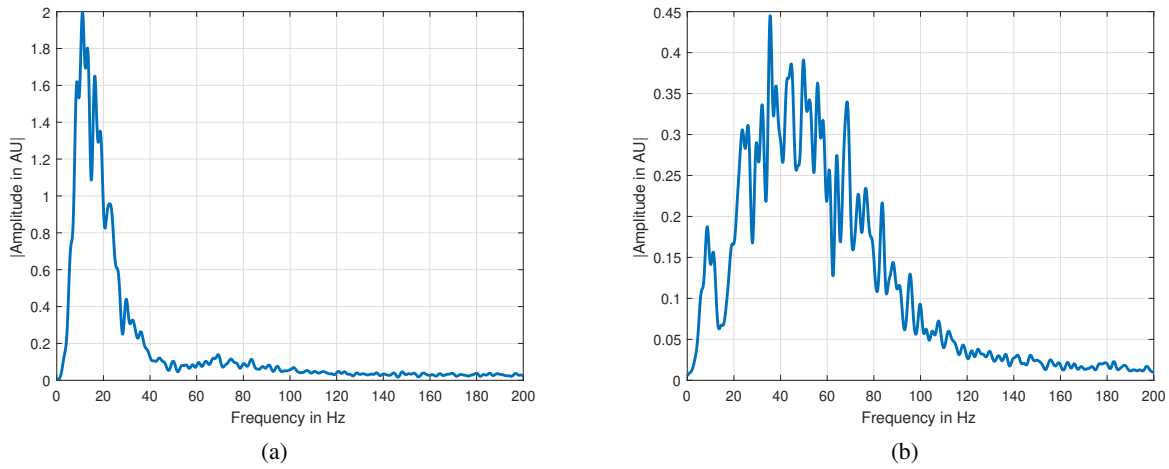
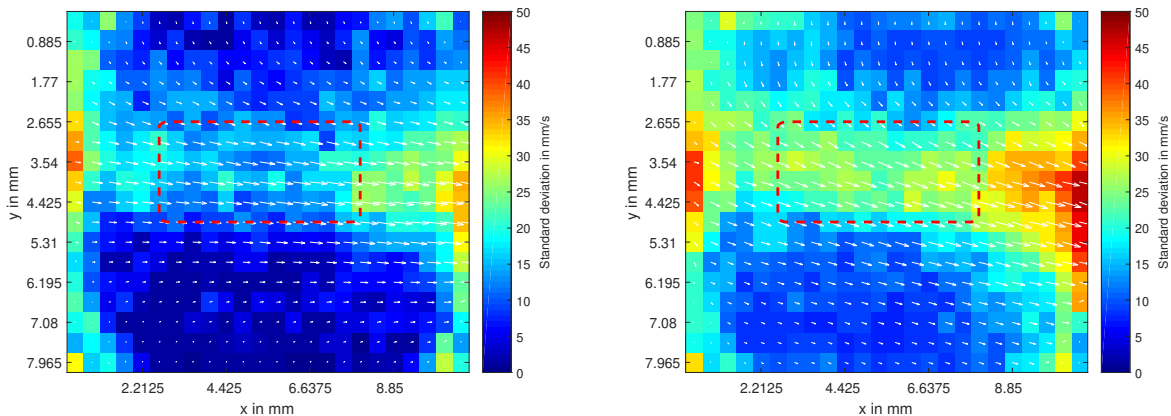
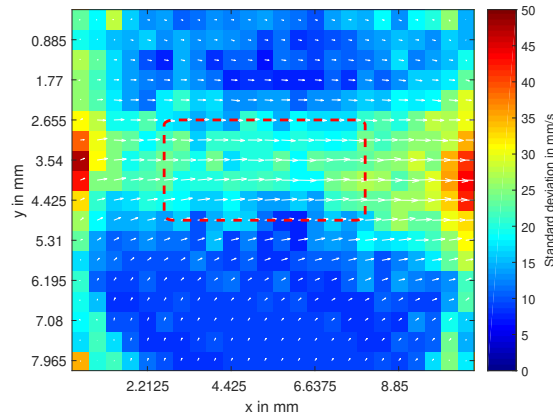


Figure 5: The figures show the amplitude spectrum of the optical distortion induced by an air flow directed on the surface. Fig. 5(a) shows the amplitude spectrum of Zernike Noll-index Z1, which corresponds to a surface tilt. Fig. 5(b) shows the amplitude spectrum of Zernike Noll-index Z7, which corresponds to a vertical coma, where distortions of up to 170 Hz are induced.

Fig. 6 shows the performance of the wavefront correction system. The flow was measured directly behind the nozzle, shown in fig. 2. The white arrows indicate the flow velocity and the background color the local standard deviation. The mean standard deviation is calculated inside of the red marked area. In fig. 6(a) the control loop and the air flow are switched off. This case serves as a reference to estimate the lowest reachable $\sigma_{mean} = 14.1$ mm/s for this setup. In fig. 6(b) the air flow directed on the surface is switched on to induce an optical fluctuating distortion, which increases the σ_{mean} to 22.3 mm/s and also induces a systematic flow field deviation. In fig. 6(c) the active control loop can decrease the standard deviation to about 18.4 mm/s and the systematic deviation is compensated. The reference uncertainty is not reached, because only low-order Zernike up to Noll-index Z4 are corrected at the moment. In the future we plan to improve the Zernike decomposition of the Hartmanogramm to correct for distortions up to Noll-index 14 to further reduce the standard deviation.



(a) Control loop and distortion (air flow) are switched off. (b) Distortion (air flow) is switched on and the control loop is off.



(c) Control loop and distortion (air flow) are switched on.

Figure 6: The figures show the performance of the control loop. The white arrows visualize the flow field mean velocity and the background color the local standard deviation.

4 Conclusion

In this contribution we show that wavefront correction systems can significantly improve PIV measurements through fluctuating phase-boundaries. The standard deviation of the mean flow, induced by an air flow stimulated fluctuating air-water interface with frequencies of up to 170 Hz, could be reduced by 47%. This uncertainty reduction can be valuable for the optical metrology community where wavefront distortions significantly degrade or prohibit the measurement. To further reduce the deviation it is planned to improve the Zernike decomposition of the Hartmanogramm to correct for distortions up to Noll-index 14. Furthermore there is the opportunity to measure the distortion of a fluctuating interface with the Fresnel Guide star method Radner et al. (2015) Radner et al. (2018a). With this technique it is not necessary to have a guide star behind the surface and only a single optical access is needed. This could be a benefit for e.g. the investigation of flow fields inside of droplets on opaque surfaces Seiler et al. (2018) e.g. chemical active surfaces in fuel cells Burgmann et al. (2017) to improve their efficiency or to investigate the flow field inside of thin cooling film flows to decrease the thermal resistance.

Acknowledgements

The authors would like to thank the DFG for funding within a Reinhart Koselleck project (DFG, grant CZ 55/30).

References

- Büttner L, Leithold C, and Czarske J (2014) Advancement of an interferometric flow velocity measurement technique by adaptive optics. *International Journal of Optomechatronics* 8
- Burgmann S, Barwari B, Maurer T, and Janoske U (2017) Hydrodynamische Instabilitäten eines Tropfens auf einer Platte unter Anströmung und Vibration. in *25. Fachtagung für Experimentelle Strömungsmechanik, Karlsruhe, Germany*
- Büttner L, Leithold C, and Czarske J (2013) Interferometric velocity measurements through a fluctuating gas-liquid interface employing adaptive optics. *Opt Express* 21:30653–30663
- Radner H, Büttner L, and Czarske J (2018a) Interferometric velocity measurements through a fluctuating interface using a fresnel guide star-based wavefront correction system. *Optical Engineering* 57:57 – 7
- Radner H, Büttner L, and Czarske J (2015) Interferometric velocity measurements through a fluctuating phase boundary using two fresnel guide stars. *Opt Lett* 40:3766–3769
- Radner H, Teich M, Büttner L, and Czarske J (2018b) FPGA-accelerated online correction of optical distortions in PIV measurements. in *19th International Symposium on the Application of Laser and Imaging Techniques to Fluid Mechanics, Lisbon, Portugal*
- Schlüßler R, Czarske J, and Fischer A (2014) Uncertainty of flow velocity measurements due to refractive index fluctuations. *Optics and Lasers in Engineering* 54:93 – 104
- Seiler P, Roisman I, and Tropea C (2018) Shear driven drop propagation and breakup on a solid substrate. in *14th International Conference on Liquid Atomization and Spray Systems, Chicago, USA*
- Willert C, Hassa C, Stockhausen G, Jarius M, Voges M, and Klinner J (2006) Combined PIV and DGV applied to a pressurized gas turbine combustion facility. *Measurement Science and Technology* 17:1670–1679